10th International Workshop on Wave Hindcasting and Forecasting, Turtle Bay, Hawaii, 2007.

THE 2007 RELEASE OF WAVEWATCH III [1]

Hendrik L. Tolman[2]

NOAA / National Centers for Environmental Prediction
Environmental Modeling Center
Marine Modeling and Analysis Branch
Camp Springs, Maryland, USA

1 INTRODUCTION

For a decade, the WAVEWATCH III wind wave model has been used for wave forecasting and hindcasting. The first public release was model version 1.18 (Tolman, 1999). A second release was model version 2.22 (Tolman, 2002c). This is presently still the most recent public release. This model version is described in detail in Tolman (2002a,b, 2003b) and Tolman et al. (2002).

Since 2002, the development of WAVEWATCH III has been ongoing. Some of this development has been documented in Tolman (2006). Earlier upgrades include model I/O suitable for non-parallel file systems on clusters (Tolman, 2003a) and a model version with a continuously moving grid (Tolman and Alves, 2005). The latter two modification have been made available in a limited release (model version 3.04), for users having to work on non-parallel file systems.

The main new development in WAVEWATCH III is the introduction of the mosaic or multi-grid approach to wave modeling. In this approach, and arbitrary number of grids with arbitrary resolutions is considered simultaneously, with continuous (two-way) data exchange between grid. This mosaic of grids thus in effect becomes a single wave model. The mosaic approach was already discussed in some detail in Tolman (2006), and will be discussed here in Section 2.

Additional upgrades of WAVEWATCH III are the introduction of new source term packages (Section 3), new output parameters, in particular the wave field partitioning throughout the spectral grid (Section 4) and various minor modifications as described in Section 5. Some changes will be made to the way in which the model code is made available. This is discussed in Section 6. Finally, an outlook to the future of WAVEWATCH III is given in Section 7.

2 THE MOSAIC APPROACH

In the mosaic approach, a number of grids with various resolutions is considered with full two-way interaction between grids. A detailed description of the development of this approach can be found in Tolman (2006, 2007, 2008). Considering the detailed description provided in the above papers, only a brief description will be given here.

In the mosaic approach, grids are identified by their rank. Grids with lower ranks have lower resolutions, while grids with identical rank have similar, but not necessarily identical resolutions. Two different types of interactions are considered between grids. For grids with different ranks, a two-way nesting approach is introduced. The first part of this two-way nesting approach provides boundary data from a low-resolution grid to a high resolution grid. This represents the traditional one-way nesting approach as used in many wave models, and is illustrated in Fig. 1. Two-way nesting is achieved by averaging spectral wave data from a high resolution grid over grid boxes of a low resolution grid and introducing these data into the low resolution grid for all grid points in such a grid that are covered by a higher resolution grid. This method is illustrated in Fig. 2.

[1] MMAB contribution Nr. 262
[2] E-mail:Hendrik.Tolman@NOAA.gov

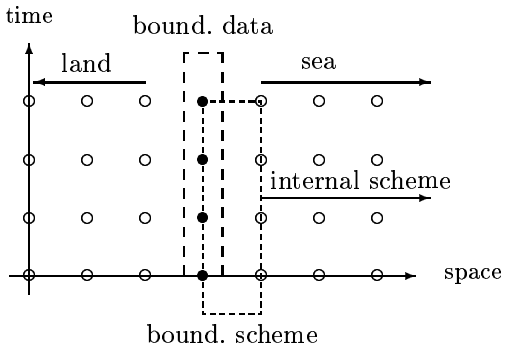

Fig. 1: Traditional one-way nesting approach as used in present and previous versions of WAVEWATCH III. One-dimensional representation in space and time, symbols represent grid points (from Tolman, 2006).

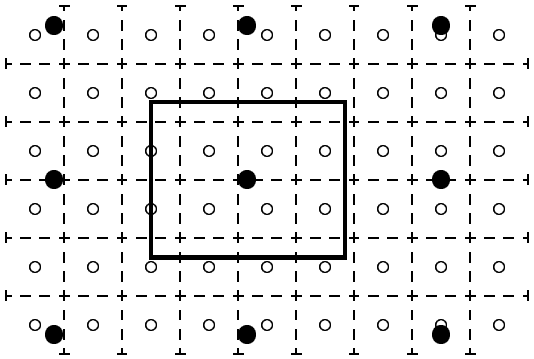

Fig. 2: Concept for reconciling lower ranked grid with higher ranked grid in two-way nesting approach. ∘ and hashed lines represent the higher ranked grid points and grid boxes, respectively, • and solid lines represent lower ranked grid and central grid box (from Tolman, 2006).

A special situation occurs when grids with identical rank (similar resolution) overlap. This is illustrated in Fig. 3. For grid 1 (∘ in Fig. 3) two areas can be distinguished. In area C, the influence of the boundary has propagated into the grid since the last reconciliation. In areas A and B, information from the boundary has not yet penetrated, and this area can be considered as the 'interior' of grid 1. Similarly, area A represents the boundary penetration depth for grid 2 (• in Fig. 3) whereas B and C represent the interior of grid 2. A simple and consistent reconciliation between grid 1 and 2 uses data from grid 1 exclusively in area A (interpolating data from grid 1 to grid points in grid 2 as necessary), and uses data from grid 2 exclusively in area C. In area B, where interior parts of both grids overlap, a consistent solution can be found by using weighted averages from both grids.

Note that this two-way nesting approach and the grid reconciliation approach do not require integer ratios of model resolutions or coinciding grid axes.

The mosaic approach requires an algorithm to automate the wave model computations for all individual grids as well as the data flow between the grids. Such an algorithm was discussed in Tolman (2006) and its necessary steps are reproduced in Fig. 4. For a detailed description of the algorithm, reference is made to the above papers.

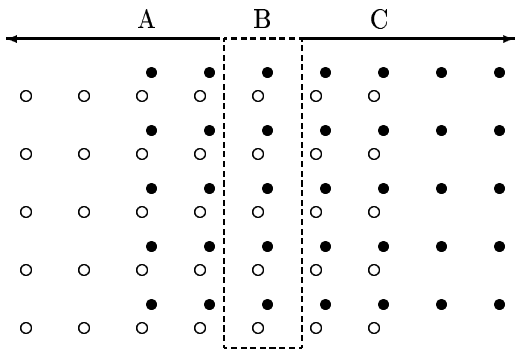

Fig. 3: Concept for reconciling grids with identical rank and therefore similar resolution. ∘ represents points of grid 1, • represents grid 2 (from Tolman, 2006).

step	action
1	Update external input
2	Update input from lower ranked grids
3	Update time step for grid
4	Run wave model for grid (no output)
5	Reconcile with grids with same rank
6	Reconcile with grids with higher rank
7	Data assimilation for grid
8	Run wave model (output only)

Fig. 4: Consecutive steps to be completed for each individual grid, defining the algorithm that controls the multi-grid wave model driver (from Tolman, 2006).

Several examples applications of the mosaic approach are given in Tolman (2006), including swell propagation through an annular current ring, nested hurricane wave modeling with the moving grid approach of Tolman and Alves (2005). Additional examples can be found in Tolman (2007), and it's application to NCEP's new operational wave model set up is presented in Chawla et al. (2007). Considering the plethora of examples presented already, no additional examples of the mosaic approach will be provided here.

3 NEW PHYSICS

In the previous releases of WAVEWATCH III, the following spectral action balance equation is solved

$$\frac{DN}{Dt} = S_{in} + S_{nl} + S_{ds} + S_{bot} \quad , \qquad (1)$$

where N represents the spectral action density and S_{in}, S_{nl}, S_{ds} and S_{bot} are source terms for wind-wave interaction, nonlinear (quadruplet) wave-wave interactions, whitecapping dissipation and wave-bottom interactions (bottom friction), respectively. In the new release of WAVEWATCH III, the right hand side of this equation is expanded

$$\begin{aligned} \frac{DN}{Dt} \quad = \quad & S_{ln} + S_{in} + S_{nl} + S_{ds} + \\ & S_{bot} + S_{db} + S_{tr} + S_{sc} + S_{xx} \quad , \end{aligned} \qquad (2)$$

where a linear input term (S_{ln}), a depth-limited breaking term (S_{db}), a triad-interaction term (S_{tr}), and a bottom scattering term (S_{sc}) have been added. Also added is a unclassified source term (S_{xx}) that can be used by users to add new physics processes. Note that the model has been prepared for triad interactions, but that presently no triad interaction source term is available. Available new source terms are discussed briefly below. Here only a brief description will be given. For a more in-depth description, reference is made to the manual of the new model release (in preparation).

3.a Linear input

In previous versions WAVEWATCH III depended on a seeding algorithm to initiate wave growth from quiescent conditions. In the new model release, a conventional linear input term is provided as an alternative to the seeding algorithm. The parameterization is based on Cavaleri and Malanotte-Rizzoli (1981), with a filter for low-frequency energy as introduced by Tolman (1992). The original filter was a function of the Pierson-Moskowitz frequency f_{PM} only. In the present implementation, the filter frequency also scales with the cut-off frequency of the prognostic computations f_{hf}. Addition of the dependency on f_{hf} assures consistent growth behavior at all fetches, without the possibility of low-frequency linear growth to dominate at extremely short fetches.

3.b Input and dissipation

The new release of WAVEWATCH III will include the input and dissipation source terms of WAM cycle 4. The input is based on the wave growth theory of Miles (1957), modified by Janssen (1982), and parameterized by Janssen (1991). The corresponding dissipation represents a modification of the WAM cycle 3 dissipation term (Komen et al., 1984) as introduced by Janssen (1994).

Various modifications to these source terms are also available. First, further developments of the ECWAM model have been included. Particularly, effects of gustiness from Abdalla and Bidlot (2002) and modifications to the dissipation term from Bidlot et al. (2005) have been included. Second, a saturation based dissipation component is available which loosely follows the proposed saturation form of Phillips (1984). Third, a negative input corresponding to Tolman and Chalikov (1996) is available. Depending on user-defined parameter settings, this package can reproduce the original WAM cycle 4 physics, ECWAM settings, and several other options.

These parameterizations have been provided by Fabrice Ardhuin of the Service Hydrographique et Océanographique de la Marine (SHOM).

3.c Nonlinear interactions

One of the methods available in WAVEWATCH III to compute four-wave nonlinear interactions is the so-called Webb-Resio-Tracy method (WRT), which is based on the original six-dimensional Boltzmann integral formulation of Hasselmann (1962, 1963a,b), and additional considerations by Webb (1978), Tracy and Resio (1982) and Resio and Perrie (1991). This method has been implemented in WAVEWATCH III using the portable subroutines developed by Van Vledder (2002). In the present release of the model, version 4 of this package is available. In the new model release, the package will be upgraded to version 6. These parameterizations have been provided by Gerbrant van Vledder of the Alkyon and Delft University of Technology.

3.d Depth-limited breaking

With increasing resolutions of applications of WAVEWATCH III, shallow water coastal areas become more and more resolved, even in operational applications (e,g, Chawla et al., 2007). This makes it essential to include surf-zone physics in the wave model to assure realistic wave conditions in the model. The most critical mechanism to include is surf-zone or depth-induced breaking, since this provides the dominant mechanism to limit shallow water wave heights. In the new model release, the approach of Battjes and Janssen (1978) has been implemented, with a limiting wave height either based on a wave height to depth ratio, or on a Miche-type criterion (Miche, 1944).

It should be noted that surf-zone physics, particularly depth-induced breaking, operate on much smaller time scales than deep water and limited-depth physics outside the surf zone. To assure reasonable behavior for larger time steps, an additional optional limiter has been adopted from the SWAN model. This limiter can be based either on a simple maximum wave height to water depth ratio, or on a Miche-style wave steepness criterion, and is optional in the model.

These parameterizations have been provided by Henrique Alves of Metocean Engineers.

3.e Bottom scattering

Waves propagating over a sloping bottom are partially reflected. If bottom depth variations are small compared to the mean water depth, the reflection coefficient is proportional to the bottom spectrum (Kreisel, 1949) and leads to a redistribution of wave energy in direction. This process may be formulated as a source term, which leads to accurate reflection coefficients when considering the evolution of the spectrum over scales larger than the bottom autocorrelation length (Ardhuin and Magne, 2007). An experimental version of Ardhuin and Magne (2007) is available in the new model version. This parameterization has been provided by Fabrice Ardhuin of SHOM.

4 NEW OUTPUT

In the new model release of WAVEWATCH III, several new output options are included. Some new output fields are available, including interaction parameters such as radiation stresses and near-bottom wave characteristics. Furthermore, friction velocities are now defined as vectors, no longer implicitly assuming that stresses are aligned with the wind direction. However, the most important addition of output parameters is the partitioning of wave spectra during run time for all grid points or for a subset of the grid, and model output based upon this partitioning.

The partitioning algorithm separates a spectrum in a set of individual wave fields. This approach was introduced by Gerling (1992). In WAVEWATCH III, the partitioning is performed using a digital image processing watershed algorithm (Vincent and Soille, 1991) first prototyped by Hanson and Jensen (2004) for the analysis of ocean wave data. Calculation of parameters for each spectral partition can then be accomplished and wave system analysis as described in Hanson and Phillips (2001) can be applied. The partitioning codes have been provided by Barbara Tracy of the US Army Corps of Engineers, Engineer Research and Development Center (USACE-ERDC).

The partitioning of spectral data results in several new output options. First, spectra for point output can be processed in this way, resulting in a file with mean wave parameters for all spectral partitions and for the spectra requested in the output post-processing program. Alternatively, these data can be generated for the entire spatial model grid or a subset thereof, as a new output option of the wave model. Finally, partitioned results can be produced as new field output options. Available are wave height, peak period and wave length, mean direction and directional spread of the wind sea, and of the first two swell fields (locally selected based on the wave height of the swell field). Additional output fields consist of the number of partitions found in the spectrum, and the total fraction of wave energy in the spectrum that is designated as being wind-driven. Note that, ideally, partitioned data are used to track individual wave fields in space and time. Such a capability is presently being developed by at USACE-ERDC.

The potential of the partitioned field output is illustrated here with some examples for the new operational model setup at NCEP. This model setup is described in detail in Chawla et al. (2007). It sufficeth to mention here that this is a global model setup. For the computations performed here, the month of January 2006 is considered only, starting the model from calm conditions.

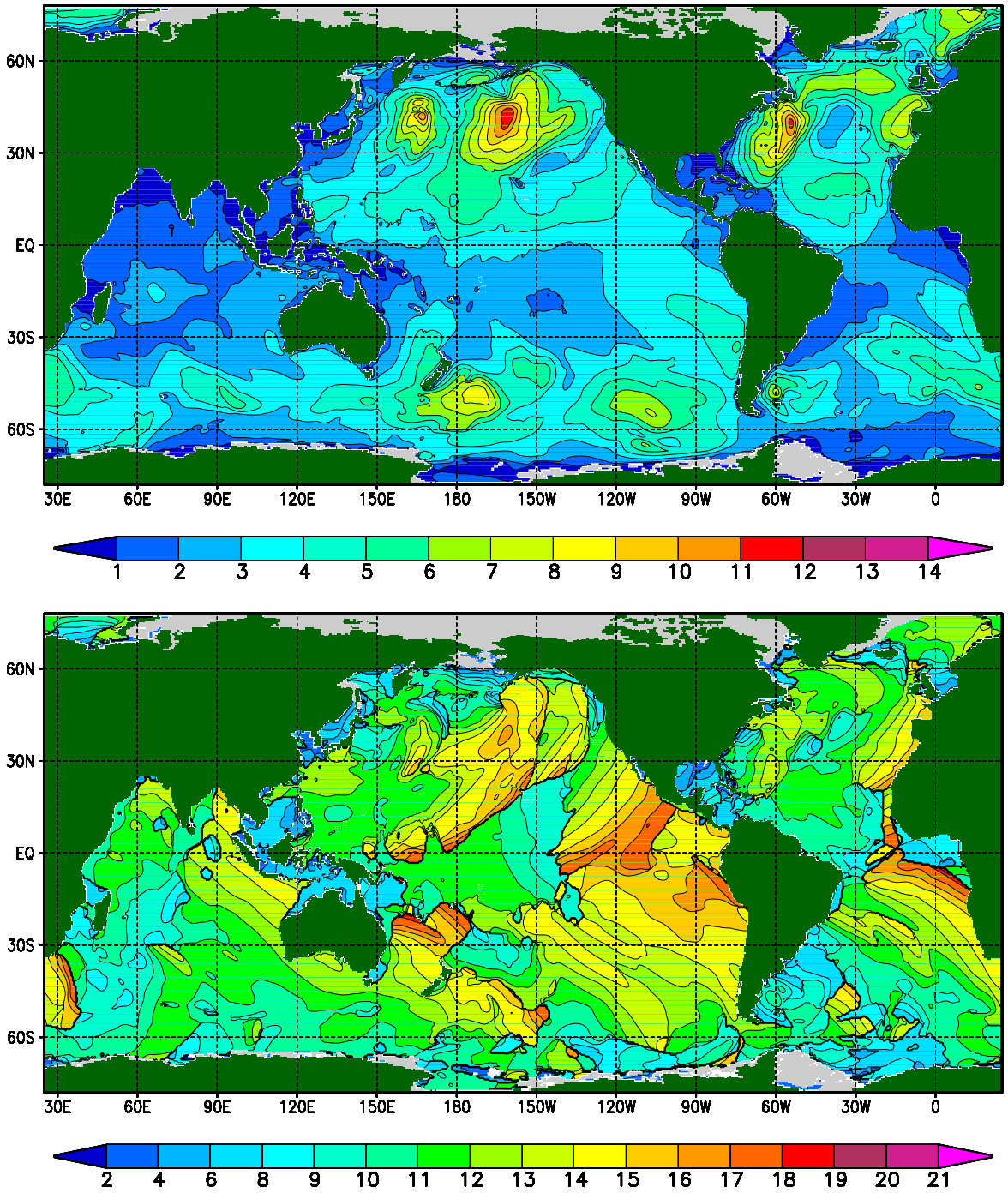

Fig. 5: Significant wave heights H_s in meters (upper panel) and peak periods T_p in seconds (lower panel, from one-dimensional frequency spectrum) from NCEP's new operational model set up for January 16 2006, 1200 UTC.

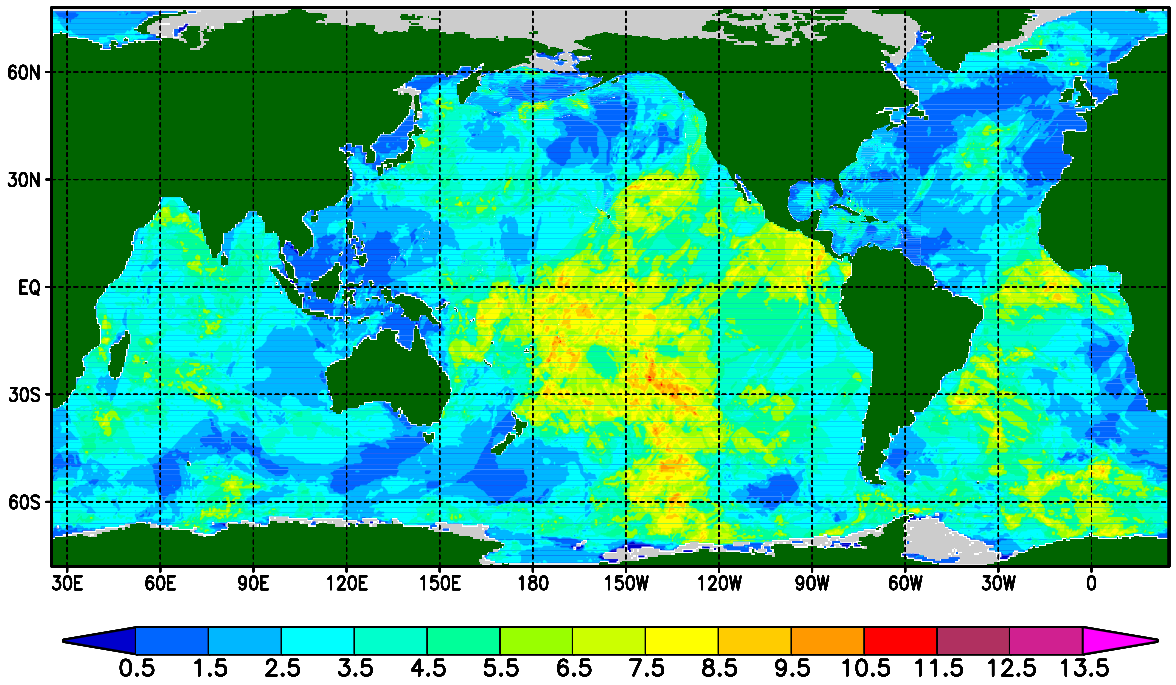

Fig. 6: Number of wave fields in NCEP's new operational model set up found by the partitioning algorithm for January 16 2006, 1200 UTC.

Figure 5 (upper panel) presents significant wave heights H_s in meters from a hindcast with this model setup valid for January 16 2006, 1200 UTC. Note that it takes approximately two weeks to spin up Pacific swells properly in this model. Hence, the model is spun up completely for this date, in spite of starting the model without prior wave conditions on January 1 2006. This figure shows the typical wave height distribution over the globe, with the most extreme wave heights concentrated at higher latitudes in storm tracks, and less extreme but notable wave heights in the tropical waters. The lower panel of this figure shows the corresponding peak wave period T_p based on the one-dimensional wave energy spectrum $F(f)$. Away from the dominant storm systems, swell fields show a typical dispersion pattern of swells, with longer and faster wave components leading shorter and slower wave components.

Figures 6 through 9 present model results obtained with the new partitioning scheme and particularly with the new field output options associated with it.

Figure 6 presets the number of individual wave fields (partitions) as identified by the partitioning scheme. In the high latitude storm tracks, only a small number of wave fields are generally identified. Near the extreme wave heights associated with storms as identified in Fig. 5, the local wave generation 'absorbs' most or all other wave fields, resulting in typically less than three individual wave fields to be identified. In manly locations, only the wind sea is identified. Conversely, wave conditions in tropical waters are dominated by swells generated at higher latitudes. In these waters, many swell systems coexist. In the tropical Pacific ocean, more than ten individually wave systems are routinely identified.

Figure 7 shows wind seas corresponding to the conditions of Fig. 5, as isolated using the partitioning scheme. Note that wind seas are defined in the wave model only when local winds are sufficiently strong to generate a wave spectrum that is resolved by the discrete frequency grid. Hence, areas where no data are presented in this figure correspond to low wind speed areas. The wave heights in the upper panel of Fig. 7 identify the high-latitude storm conditions that dominate the extreme wave heights in Fig. 5 as would be expected. The wind sea partition also identifies persistent wind seas associated with persistent tropical ind systems such as the trade winds. Note that these wind seas are not clearly identifiable in the overall wave heights of Fig. 5, because of the large or even dominant swells in these areas. The peak periods associated with wind seas (lower panel in Fig. 7) are related to local forcing only, and hence

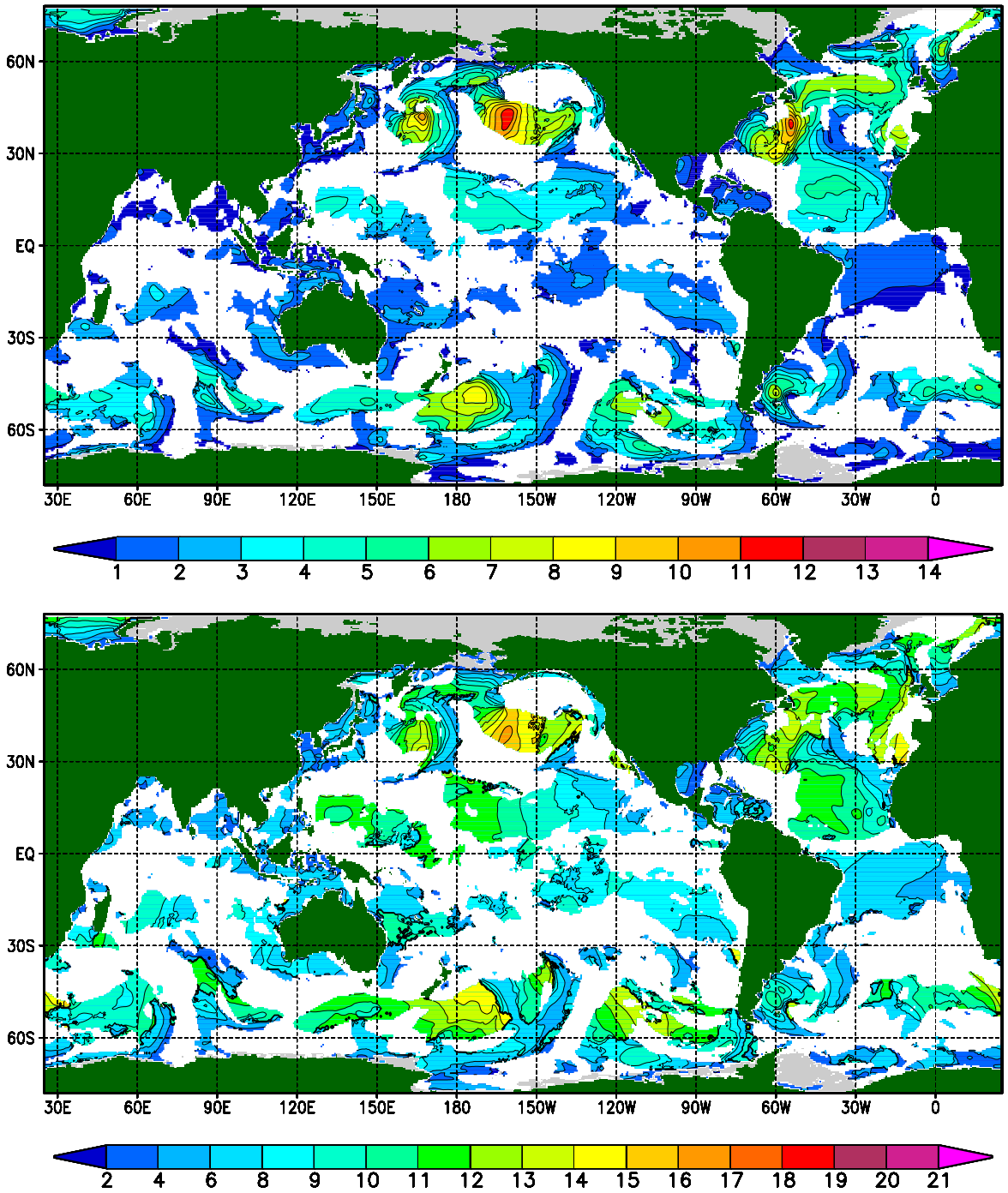

Fig. 7: Wind sea parameters in NCEP's new operational model set up found by the partitioning algorithm for January 16 2006, 1200 UTC. Upper panel shows wave heights H_s in meters, lower panes shows wind sea peak periods in seconds.

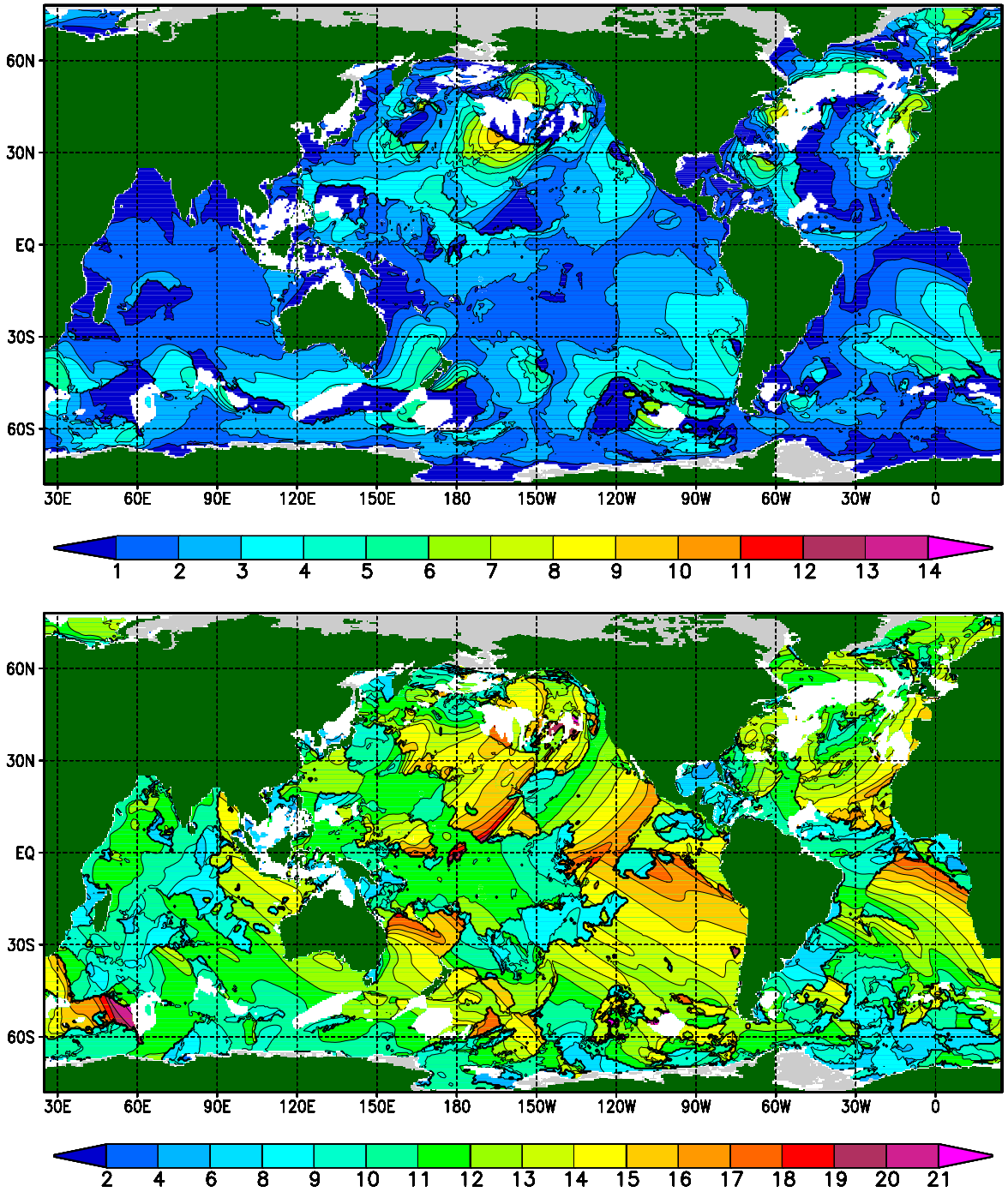

Fig. 8 : Like Fig. 7 for primary swell.

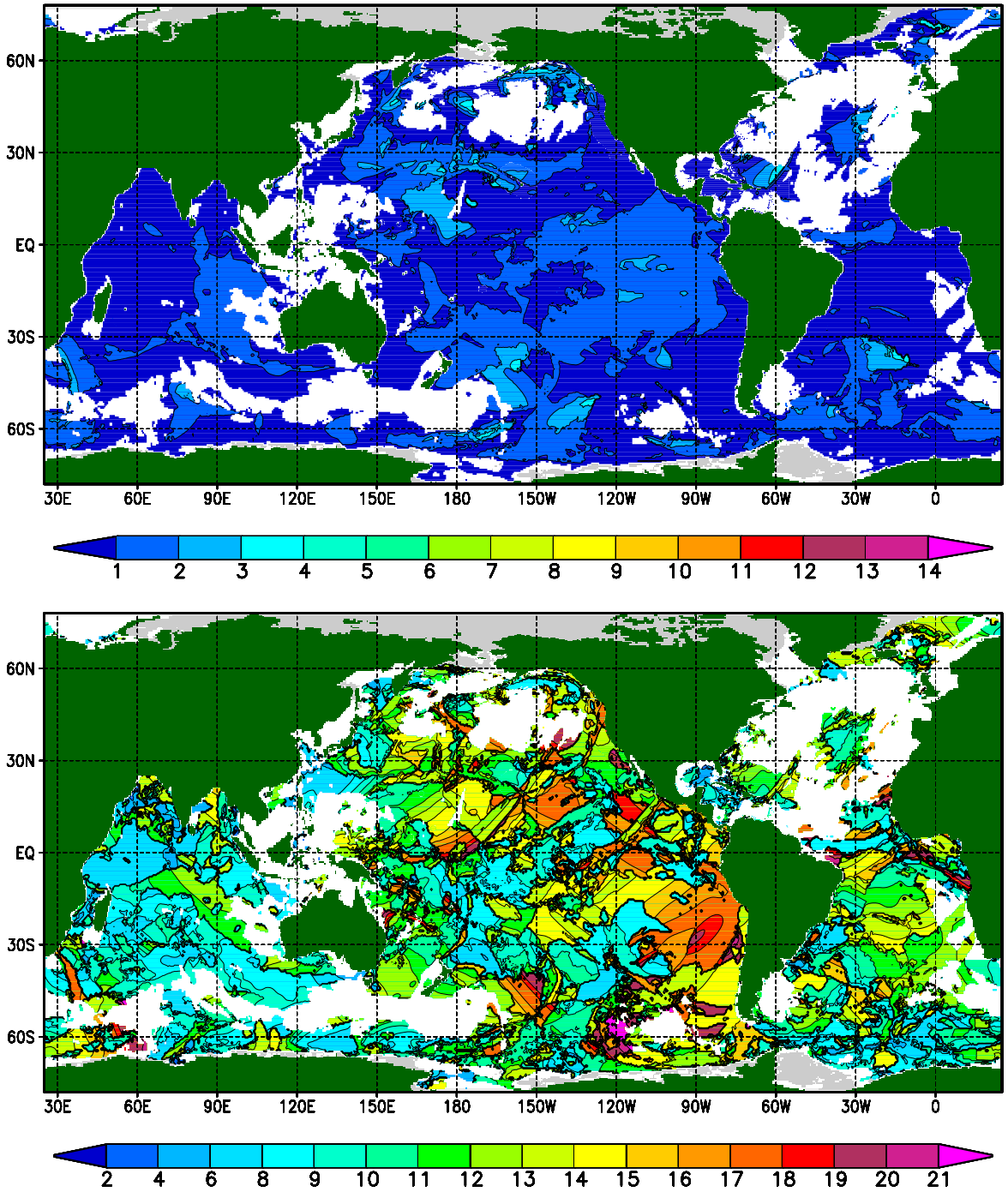

Fig. 9 : Like Fig. 7 for secondary swell.

do not show dispersion patterns.

Figure 8 shows the corresponding primary or dominant swells. Note that no swells are identified in areas where only a dominant wind sea exists (compare to Figs. 5 and 7). Some of the highest primary swell wave heights occur next to the highest wind sea wave heights, and thus represent a transition from swell to wind sea. Note that this transition is always somewhat arbitrary, as it involves a cut-off fraction of wave energy driven by local winds. The corresponding peak periods (lower panel of Fig. 8) show the clear dispersion pattern as also unidentified for the overall peak period in Fig. 5. A comparison of in particular the wave periods between the wind seas and primary swells (Figs. 7 and 8) clearly illustrated the differences in dispersion behavior between the two wave system types.

Finally, Fig. 9 displays the secondary swell fields. Characteristics are similar to those of the primary swell fields, however, the fields are more chaotic and less consistent. This is mainly due to the fact that the swell fields are selected based on the local rank in wave height only. The fact that even these fields contain clearly consistent areas suggests that much more consistent results can be obtained if individual swell fields are tracked in space and time, using three dimensional clustering techniques similar to those used by Hanson and Phillips (2001) for buoy observations.As mentioned above, such techniques are being developed at USACE-ERDC.

5 OTHER UPDATES

Most major model modifications have been discussed above. Some minor modifications include:

- GrADS scripts for plotting spectra and source terms have been refined to allow both color and black and white plots, and for Cartesian or polar representation of the frequency-direction space.

- A distinction is now made between land points and otherwise excluded grid points. Active boundary points can now be located at the outer grid boundaries, without the necessity for these points to be land points. This approach makes it possible to carve out arbitrary computational domains from an otherwise conventional rectangular computational grid.

- In the mosaic approach spectral resolutions now may vary between grids. Interpolations between grids are performed inside the model as needed.

6 MODEL DISTRIBUTION

Previous versions of WAVEWATCH III have been distributed through NCEP's web site[3] as a manual, a set of tar files and an installation program. The new model version will initially be distributed in the same fashion. However, to facilitate collaboration in development of the model, we intend to distribute the new model version as open source software. The exact licensing details are still under discussion at NCEP. In this approach, we intend to distribute the code on several subversion (Collins-Sussmann et al., 2004) servers. On one server, developmental codes will be available for collaborators. Another server will be used to distribute formal model releases and bug fixes and other upgrades for the officially distributed model versions. The first server will feature password controlled access only, with access to be granted to those who intend to collaborate on code development, or who have code to contribute. The second server will be open to the public, and is intended to become the formal distribution site of the WAVEWATCH III codes. NCEP will at least initially retain control over the subversion servers and all updates to the code. Details on the new model distribution methods will be posted on the NCEP web site[3].

Also considered for distribution are tools that can be used with WAVEWATCH III. A good example of this is the grid generation code of Chawla and Tolman (2007, 2008). Other tools that will be considered or distribution are Matlab routines for model data processing and tools for packing model output in standard formats (GRIB, GRIB2, NetCDF, etc.).

7 OUTLOOK

From its inception, the WAVEWATCH III model code has been designed as a modeling framework; the model has a high level of plug-compatibility with respect to numerical and physical approaches, and optimization, parallelization and mosaic approaches are kept separate from the numerical and physical approaches. With the availability of more source term options, WAVEWATCH III has truly become

[3] http://polar.ncep.noaa.gov/wavewatch

a modeling framework. For instance, models run at NCEP, SHOM (Fabrice Ardhuin) and several research models based on the WRT nonlinear interaction routines, all are distinctly different wave models contained within the WAVEWATCH III framework.

A modeling framework can only be effective is it is freely available to those who want to use it to develop their wave modeling concepts. For this reason, the WAVEWATCH III source code has always been freely available. This has already led to several contributions to the source code from outside NCEP. Many of these contributions are documented in this paper. The move to developing the framework further in an open-source environment is made to further facilitate the use and joint development of WAVEWATCH III.

The joint development of WAVEWATCH III is accelerating. Various new grid approaches are being developed, including generalized curvilinear grids, and unstructured grid approaches according to Hsu et al. (2005). A wrapper for the wave model is developed to make it compliant with the Earth System Modeling Framework (ESMF). Various NetCDF packing approaches are being developed for model output. Several new source term, particularly for shallow water, are being developed or ported from other wave models. All these future model upgrades are developed outside NCEP, but each of these modifications is intended for future operational implementation at NCEP.

At NCEP further development of WAVEWATCH III is also ongoing. The main focus is on coupled ocean-wave-atmosphere modeling for hurricanes. Various new numerical and model physics parameterizations are at various levels of development, and will be included in the wave model as they reach sufficient maturity.

With the accelerated rate of development of WAVEWATCH III, and with the new model distribution methods that are being designed and implemented, it is expected that new releases of WAVEWATCH III will become much more frequent than in the past.

References

Abdalla, S. and J. R. Bidlot, 2002: Wind gustiness and air density effects and other key changes to wave model in CY25R1. Tech. Rep. Memomrandum R60.9/SA/0273, Research Department, ECMWF, Reading, U. K.

Ardhuin, F. and R. Magne, 2007: Current effects on scattering of surface gravity waves by bottom topography. *J. Fluid Mech.*, **576**, 235–264.

Battjes, J. A. and J. P. F. M. Janssen, 1978: Energy loss and set-up due to breaking of random waves. in *Proc. 16th Int. Conf. Coastal Eng.*, pp. 569–587. ASCE.

Bidlot, J. R., S. Abdalla and P. A. E. M. Janssen, 2005: A revised formulation for ocean wave dissipation in CY25R1. Tech. Rep. Memorandum R60.9/JB/0516, Research Department, ECMWF, Reading, U. K.

Cavaleri, L. and P. Malanotte-Rizzoli, 1981: Wind-wave prediction in shallow water: Theory and applications. *J. Geophys. Res.*, **86**, 10,961–10,973.

Chawla, A., D. Cao, V. M. Gerald, T. Spindler and H. L. Tolman, 2007: Operational implementation of a multi-grid wave forecast system. in *10th international workshop on wave hindcasting and forecasting.*

Chawla, A. and H. L. Tolman, 2007: Automated grid generation for WAVEWATCH III. Tech. Note 254, NOAA/NWS/NCEP/MMAB, 71 pp.

Chawla, A. and H. L. Tolman, 2008: Obstruction grids for spectral wave models. *Ocean Mod.*, Submitted.

Collins-Sussmann, B., B. W. Fitzpatrick and C. M. Pilato, 2004: *Version control with subversion.* O'Reilly, 320 pp.[4]

Gerling, T. W., 1992: Pattitioning sequences and arrays of directional ocean wave spectra into component wave systems. *J. Atmos. Oceanic Techn.*, **9**, 444–458.

Hanson, J. L. and R. E. Jensen, 2004: Wave system diagnostics for numerical wave models. in *8^{th} international workshop on wave hindcasting and forecasting, JCOMM Tech. Rep. 29, WMO/TD-No. 1319.*

Hanson, J. L. and O. M. Phillips, 2001: Automated analysis of ocean surface directional wave spectra. *J. Atmos. Oceanic Techn.*, **18**, 177–293.

Hasselmann, K., 1962: On the non-linear transfer in a gravity wave spectrum, Part 1. General theory. *J. Fluid Mech.*, **12**, 481–500.

Hasselmann, K., 1963a: On the non-linear transfer in a gravity wave spectrum, Part 2, Conservation theory, wave-particle correspondence, irreversibility. *J. Fluid Mech.*, **15**, 273–281.

Hasselmann, K., 1963b: On the non-linear transfer in a gravity wave spectrum, Part 3. Evaluation of

[4] Updated versions available online at http://subversion.tigris.org/.

energy flux and sea-swell interactions for a Neuman spectrum. *J. Fluid Mech.*, **15**, 385–398.

Hsu, T.-W., S.-H. Ou and J.-M. Liau, 2005: Hindcasting near shore wind waves using a FEM code for SWAN. *Coastal Eng.*, **52**, 177–195.

Janssen, P. A. E. M., 1982: Quasilinear approximation for the spectrum of wind-generated water waves. *J. Fluid Mech.*, **117**, 493–506.

Janssen, P. A. E. M., 1991: Quasi-linear theory of of wind wave generation applied to wave forecasting. *J. Phys. Oceanogr.*, **21**, 1631–1642.

Komen, G. J., S. Hasselmann and K. Hasselmann, 1984: On the existence of a fully developed windsea spectrum. *J. Phys. Oceanogr.*, **14**, 1271–1285.

Kreisel, G., 1949: Surface waves. *Quart. Journ. Appl. Math.*, pp. 21–44.

Miche, A., 1944: Mouvements ondulatoire de la mer en profondeur croissante ou décroissante. Forme limite de la houle lors de son déferlement. Application aux digues maritimes. Deuxième partie. Mouvements ondulatoires périodiques en profondeur régulièrement décroissante. *Annales des Ponts et Chaussées*, **114**, 131–164, 270–292.

Miles, J. W., 1957: On the generation of surface waves by shear flows. *J. Fluid Mech.*, **3**.

Phillips, O. M., 1984: On the response of short ocean wave components at a fixed wavenumber to ocean current variations. *J. Phys. Oceanogr.*, **14**, 1425–1433.

Resio, D. T. and W. Perrie, 1991: A numerical study of nonlinear energy fluxes due to wave-wave interactions. Part 1: Methodology and basic results. *J. Fluid Mech.*, **223**, 609–629.

Tolman, H. L., 1992: Effects of numerics on the physics in a third-generation wind-wave model. *J. Phys. Oceanogr.*, **22**, 1095–1111.

Tolman, H. L., 1999: User manual and system documentation of WAVEWATCH III version 1.18. Tech. Note 166, NOAA/NWS/NCEP/OMB, 110 pp.

Tolman, H. L., 2002a: The 2002 release of WAVEWATCH III. in *Preprints 7th international workshop on wave hindcasting and forecasting*, pp. 188–197. Environment Canada.

Tolman, H. L., 2002b: Alleviating the garden sprinkler effect in wind wave models. *Ocean Mod.*, **4**, 269–289.

Tolman, H. L., 2002c: Testing of WAVEWATCH III version 2.22 in NCEP's NWW3 ocean wave model suite. Tech. Note 214, NOAA/NWS/NCEP/OMB, 99 pp.

Tolman, H. L., 2003a: Running WAVEWATCH III on a linux cluster. Tech. Note 228, NOAA/NWS/NCEP/MMAB, 27 pp.

Tolman, H. L., 2003b: Treatment of unresolved islands and ice in wind wave models. *Ocean Mod.*, **5**, 219–231.

Tolman, H. L., 2006: Toward a third release of WAVEWATCH III; a multi-grid model version. in *9 th international workshop on wave hindcasting and forecasting, JCOMM Tech. Rep. 34, WMO/TD-No. 1368.* Paper L1.

Tolman, H. L., 2007: Development of a multi-grid version of WAVEWATCH III. Tech. Note 256, NOAA/NWS/NCEP/MMAB, 88 pp. + Appendices.

Tolman, H. L., 2008: A mosaic approach to wind wave modeling. In preparation.

Tolman, H. L. and J. H. G. M. Alves, 2005: Numerical modeling of wind waves generated by tropical cyclones using moving grids. *Ocean Mod.*, **9**, 305–323.

Tolman, H. L., B. Balasubramaniyan, L. D. Burroughs, D. V. Chalikov, Y. Y. Chao, H. S. Chen and V. M. Gerald, 2002: Development and implementation of wind generated ocean surface wave models at NCEP. *Wea. Forecasting*, **17**, 311–333.

Tolman, H. L. and D. V. Chalikov, 1996: Source terms in a third-generation wind-wave model. *J. Phys. Oceanogr.*, **26**, 2497–2518.

Tracy, B. and D. T. Resio, 1982: Theory and calculation of the nonlinear energy transfer between sea waves in deep water. WES Report 11, US Army Corps of Engineers.

Van Vledder, G. Ph., 2002: A subroutine version of the Webb/Resio/Tracy method for the computation of nonlinear quadruplet interactions in a wind-wave spectrum. Report 151b, Alkyon, The Netherlands.

Vincent, L. and P. Soille, 1991: Watersheds in digital spaces: An efficient algorithm based on immersion simulations. *IEEE Transactions of Pattern Analysis and Machine Intelligence*, **13**, 583–598.

Webb, D. J., 1978: Non-linear transfers between sea waves. *Deep-Sea Res.*, **25**, 279–298.